

Selective Laser Melting: On the Study of Microstructure of K220

Zhang, Dan Qing; Liu, Zhong Hong; Li, Shuai; Chua, Chee Kai; Muzzammil, Muhd.; Wong, C. H.

2014

Zhang, D. Q., Liu, Z. H., Li, S., Muzzammil, M., Wong, C. H., & Chua, C. K. (2014). Selective Laser Melting: On the Study of Microstructure of K220. Proceedings of the 1st International Conference on Progress in Additive Manufacturing (Pro-AM 2014), 176-184.

<https://hdl.handle.net/10356/84272>

https://doi.org/10.3850/978-981-09-0446-3_049

© 2014 by Research Publishing Services.

Downloaded on 19 Aug 2022 00:10:15 SGT

SELECTIVE LASER MELTING: ON THE STUDY OF MICROSTRUCTURE OF K220

D.Q. ZHANG¹,

¹ *NTU Additive Manufacturing Centre, School of Mechanical & Aerospace Engineering, Nanyang Technological University, HW1-01-05, 2A Nanyang Link, Singapore 637372*

Z.H. Liu¹, S. LI², Muhd. MUZZAMMIL¹, C.H. Wong¹ & C.K. Chua¹

² *State key Lab of Materials Processing and Die & Mould Technology, School of Materials Science and Engineering, Huazhong University of Science and Technology, No1037 Luoyu Road, Hongshan District, Wuhan 430074, China*

ABSTRACT: K220 copper parts were produced by Selective Laser Melting (SLM) technology. The relative densities and microstructures of the SLM parts under different laser energy densities were measured and analysed. We observed an increasing relative density when laser energy input was enlarged. However, when the laser energy density exceeded 700 J/mm³, severe balling occurred. In this work, a high relative density of 99.9 % was obtained when an energy density of 200 J/mm³ was applied. The microstructure of the SLM parts revealed cellular dendrites with dimensions of 1 μm. Two different heat treatment processes were applied and the microstructure and micro-hardness were also investigated. Laminated precipitate with dimension of 1 μm can be seen after 25 hours of age-hardening. Moreover, when the age-hardening period was increased from 12 hours to 25 hours, the micro-hardness improved from 187.9±5.2 Hv0.1 to 192±11.2 Hv0.1 in xy plane. This is due to precipitate hardening of K220 after the heat treatment process.

Keywords: Selective laser melting; K220 Copper alloy; Microstructure; Heat treatment; 3D printing

INTRODUCTION

The importance of additive manufacturing in revolutionising the manufacturing industry is akin to how nanotechnology in material science has radically changed how materials can be engineered for a specific applications. For instance, the remarkable properties of carbon nanotube (Wong and Vijayaraghavan 2014; Vijayaraghavan and Wong 2013; Wong and Vijayaraghavan 2012; Wong 2010) have endeared itself to a myriad of applications; the combination of mutually exclusive properties of strength, deformation and durability to form bulk metallic glass (Wang and Wong 2011; Wang and Wong 2012) has reign itself as a technological material of choice, and while complex parts are finding themselves being additively manufactured rather than by conventional manufacturing processes. However, widespread adoption of additive manufacturing is inhibited by the lack of suitable materials with good properties. As such, identifying new materials with good properties that can be used in additive manufacturing is of paramount importance.

Cu–Ni–Si-based alloy is a recent commonly investigated Cu-based alloy that has created considerable interest due to their high strength, thermal and electrical conductivity with vast applications in the electronic industries (Gu and Shen, 2006; Gu and Shen, 2009). The good corrosion resistance and high thermal conductivity of copper make it suitable for applications as tubes, vessels and heat exchangers in the chemical and food industries. With an increasing demand for low cost, high efficiency complex designs such as micro-heat exchangers produced in copper with a wall thickness of 100 μm (Pogson et al., 2003), there is therefore an urgent need to explore new manufacturing techniques with such capabilities.

The strengthening in these alloys is achieved due to the precipitation of finely distributed second phase particles. Electron microscopy investigations identified the precipitate particles corresponding to either Ni_2Si (Lockyer and Noble, 1994) or Ni_3Si (Srivastava et al., 2004) intermetallic phases. K220 is a kind of Cu–Ni–Si-based alloy that contains 2.4% Ni element and 0.7% Si element. Moreover, this copper alloy is heat treatable (Zhao et al., 2003). As such, the forming process of this kind of alloy should be fully understood with the aim to explore further application in industry.

Selective laser melting (SLM), which is a newly developed forming process, enables manufacturing of parts layer by layer through melting a thin layer of metal powder. This technology can be used for fabricating parts with complex geometries made up of materials such as high speed steel (Liu et al., 2013), AlSi10Mg (Loh et al., 2014), Ti alloy (Gu and Zhang, 2013) and copper alloy (Zhang et al., 2013).

This paper aims to evaluate the resultant microstructures and properties of K220 copper parts produced by the SLM technique before and after heat treatment process. The forming parameters for the copper alloy will be addressed and described. Finally, the resultant microstructure were examined and characterised. Different heat treatment processes were investigated to obtain the optimized properties. The potential applications involved in the SLM process were systematically studied through experimental studies and microstructures characterization.

EXPERIMENTAL PROCEDURE

In this study, K220 copper parts were produced with the SLM250HL machine from SLM Solutions GmbH equipped with a fiber laser of 400 W. Gas atomized pre-alloy spherical K220 powder with a particle size of 20–63 μm was used for the experiment. Parts were produced using different forming parameters, laser power, scan speed, hatch spacing, preheating temperature and layer thickness. The resultant relative densities of the produced parts were evaluated using the Archimedes principle. Samples of K220 copper alloy were prepared for metallographic examination according to standard polishing procedures and etched with a mixture of 65% HNO_3 for 5 s.

Heat treatment was carried out in two phases: (1) solution heat treatment at 900 $^{\circ}\text{C}$ for 1 hour in nitrogen followed by quenching and (2) ageing at 450 $^{\circ}\text{C}$ for 12 hours/25 hours (Srivastava et al., 2004). A micro-hardness tester was employed to determine the Vickers hardness of the SLM copper samples and also after two settings of heat treatment using a load of 100 g and an indentation time of 15 s. K220 copper parts with different features were also produced according to the optimized parameters (see figure 1). The SLM parts showed dense surfaces with a relative density of 99.9%.



Figure 1: SLM parts produced using K220 powder

RESULTS AND DISCUSSION

MICROSTRUCTURE OF K220 SLM SAMPLES

Figure 2 shows the scanning electron microscopy (SEM) images of the microstructure of the SLM parts at different magnifications. Cellular dendrites can be observed in different directions revealing the grain boundaries clearly. The dimension of the cellular dendrites showed in Figure 2d is about $1\ \mu\text{m}$. This was because SLM is characterised by rapid solidification that results in several key structural features, one of which is grain size refinement. During the process, heat flows against the scan direction and this causes the grains to crystallize along that direction of the thermal gradient.

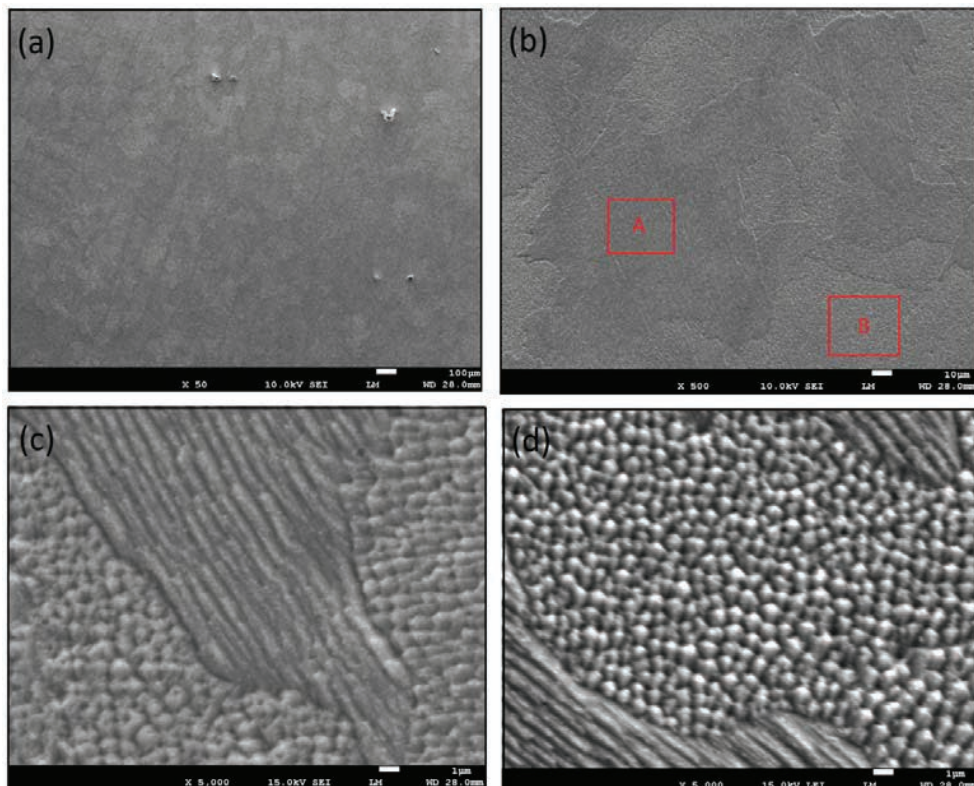


Figure 2: Typical microstructures of K220 copper alloy samples using SLM (a) and (b), high magnification of zone A (c) and high magnification of zone B (d)

Figure 3 shows the microstructure morphologies of the SLM parts after heat treatment. Figure 3a, b, and Figure 3c and d, depict the SEM images after 12 hours and 25 hours of ageing, respectively. Laminated precipitates were observed after heat treatment of under 12 hours ageing. However, as the ageing time increases to 25 hours, the precipitates grow in size of up to 1. Therefore, ageing time has a significant influence on the microstructure and the quantity and size of the precipitates increase with increasing age-hardening period. In Figure 3(b), we clearly see that the spherical precipitates are small in size after 12 hours of age-hardening, while Figure 3(d) depicts an accumulation of distinct lamellar growth of precipitates along the grain boundaries after 25 hours of age hardening.

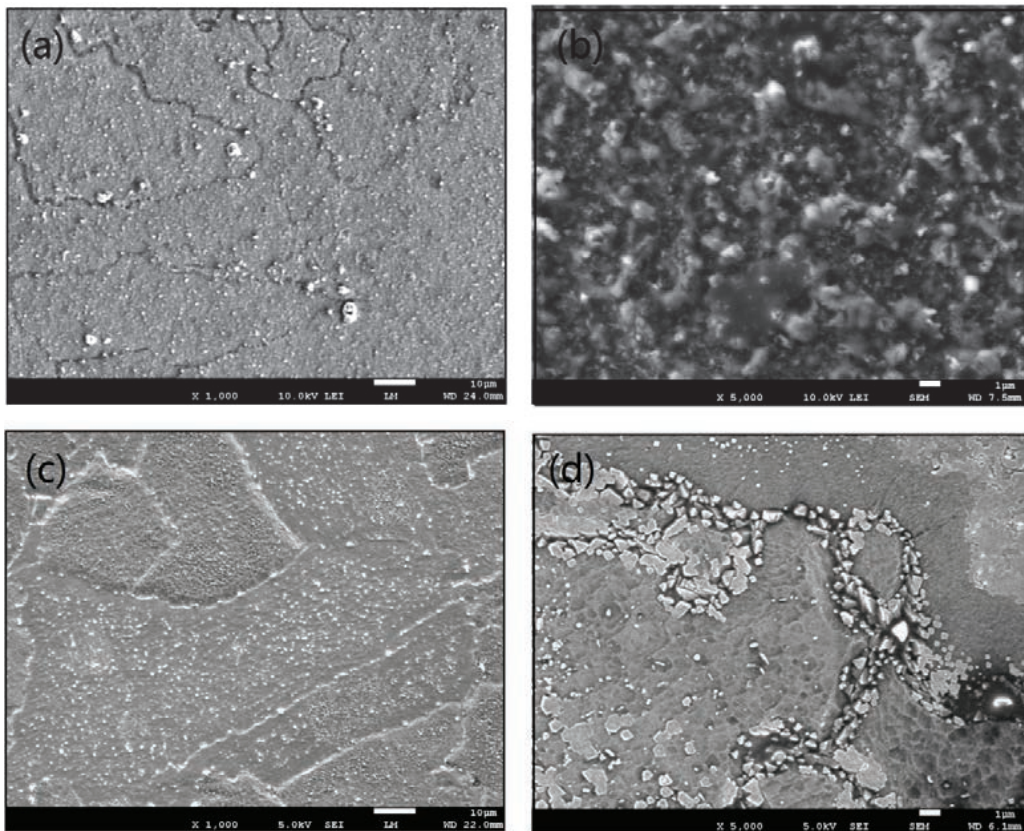


Figure 3: Typical microstructures of SLM K220 copper alloy samples after heat treatment with 12 hours age-hardening in (a)XY plane and (b)YZ plane, and 25 hours age-hardening in (c)XY plane and (d)YZ plane

Relative density versus laser energy input

Figure 4 shows the relationship between the relative density and the volumetric energy density of the SLM K220 samples. In this test, the laser power used was 375 W, hatch spacing was 0.09 mm, scan speed was 530 mm/s and layer thickness was 0.03mm. The variation in the laser energy input is due to the variation of scan speeds and hatch spacing.

From the figure, it is apparent that the increase in relative density is associated with the increase in volumetric energy density. The relative densities of the parts were observed to be higher than 98.8% for volumetric energy densities above 200 J/mm³. At higher volumetric energy density, the SLM process was inhibited due to the severe balling where it gets in the way of the recoating mechanism. This was due to the large liquid content formed during the melting process where a continuous melt track breaks into several spherical agglomerates before solidification (due to diminishing surface energy). As a result, a discontinuous balling track was formed (Gu et al., 2006).

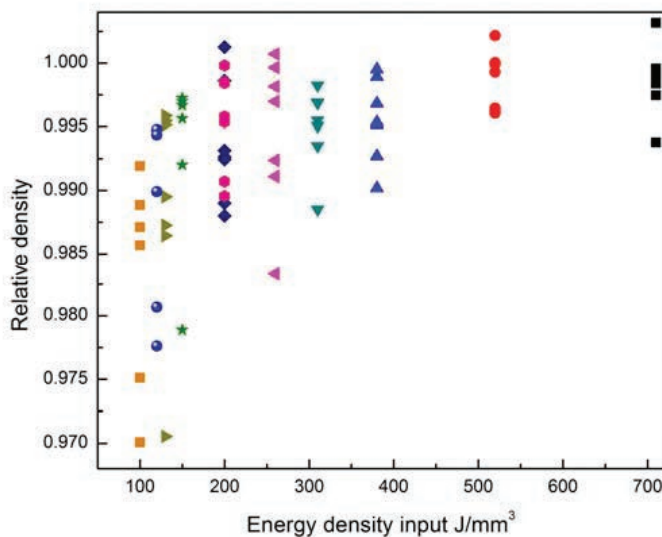


Figure 4: Relative density of SLM K220 samples against volumetric energy density

Our previous research (Zhang et al., 2013) on C18400 copper alloys showed that SLM process is sensitive to the chemical composition of copper alloys. The forming process of C18400 copper alloy was unstable and the highest relative density was around 90% while K220 copper alloy exhibits a relative density of 99.9%. The improved relative density in K220 alloys is due to the presence of Ni content which improves the absorptivity of the powder system. Figure 5 illustrates the huge difference in reflectivity between the C18400 powder and K220 powder. For instance, when the wavelength of the fibre laser is 1064 nm, the reflectance of K220 powder is $42.09 \pm 0.6\%$ compared to $59 \pm 1\%$ of the C18400 powder.

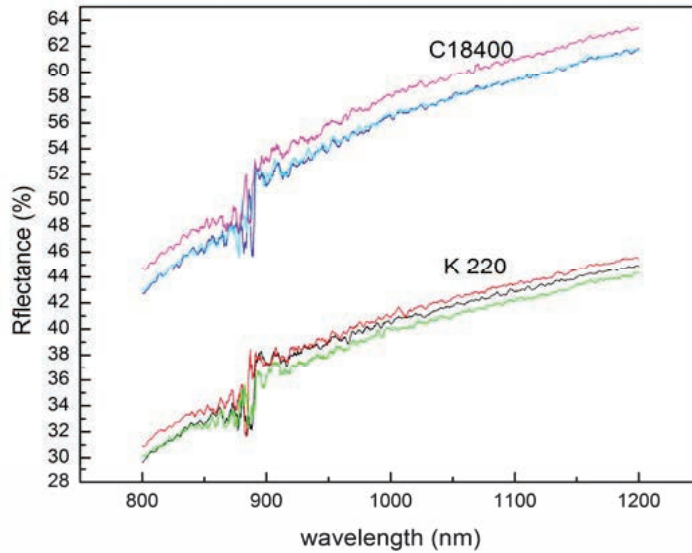


Figure 5: Reflectance of K220 and C18400 powders under different wavelength

MICRO-HARDNESS

According to literature review (Srivastava et al., 2004), the hardness value of Cu-2.4Ni-0.6Si can be increased due to the precipitates formed after age-hardening. The electrical conductivity also increases with 25 hours of age-hardening which will decrease with further age-hardening. In this work, two different heat treatment processes with 12 and 25 hours of age-hardening were carried out. The micro-hardness value was measured in order to appropriately identify proper heat treatment process.

Table 1 illustrates the micro-hardness values of SLM copper parts produced using laser power of 375 W, hatch spacing of 0.09 mm, and scan speed of 530 mm/s. The average micro-hardness value of the produced sample was $81.56 \pm 3.6 \text{HV}_{0.1}$, while the micro-hardness value of bulk K220 is 120 HV. A proper heat treatment process will therefore be needed to improve the hardness. When 25 hours of age-hardening was applied, the micro-hardness value increased to $187.9 \pm 5.2 \text{HV}_{0.1}$ (xy plane) and $184.3 \pm 5.7 \text{HV}_{0.1}$ (yz plane). However, the micro-hardness difference between 12 and 25 hours of age-hardening was not remarkable; the standard deviation of 25 hours age-hardening was also larger than other specimens.

Table 1: Micro-hardness of K220 samples (as built; heat treatment 12h; heat treatment 25h)

No.	Hardness value (as built, XY)	Hardness value (as built, YZ)	Hardness value (heat treatment 12h, XY)	Hardness value (heat treatment 12h, YZ)	Hardness value (heat treatment 25h, XY)	Hardness value (heat treatment 25h, YZ)
1	75.7	79	189	174	208	183
2	86.3	83.2	179	188	199	165
3	83.4	80.7	188	185	208	185
4	83	81.6	192	188	186	177
5	83.9	85.3	197	191	183	169
6	83.4	84.4	185	180	183	194
7	78.6	90.2	186	180	183	181
8	78.2	94	187	188	186	174
<i>Average</i>	81.56±3.6	84.8±5.0	187.9±5.2	184.3±5.7	192±11.2	178.5±9.3

CONCLUSION

The microstructure and forming process of K220 using SLM were discussed comprehensively. This work has demonstrated the possibility and further application on SLM of K220 copper alloy.

- (1) The energy density input was systematically investigated through optimization of the forming parameters. A tendency of increasing relative density was observed when the laser energy input was enlarged. High relative density of 99.9 % was obtained when applying an energy density of 200 J/mm³.
- (2) The microstructure of the as-built samples consisted of cellular dendrites. These cellular dendrites can be observed in several different directions indicating the grain boundaries clearly. The dimension of the cellular dendrites was evaluated to be about 1 μ m.
- (3) Age-hardening time has significant influence on the microstructure of the parts. The quantity and the size of the precipitates increased when age-hardening time was increased. Scanning electron microscopy images after 25 hours of ageing distinctly revealed lamellar growth of precipitates that congregate along the grain boundaries.
- (4) The average micro-hardness value of the produced sample was 81.56±3.6HV_{0.1}. When age-hardening was increased to 25 hours, the micro-hardness value increased to 187.9±5.2 HV_{0.1} in the xy plane and 184.3±5.7HV_{0.1} in the yz plane.

REFERENCES

- Gu, D. and Zhang, G., 2013. Selective laser melting of novel nanocomposites parts with enhanced tribological performance. *Virtual and Physical Prototyping*. 8, 11-18.
- Gu, D.D. and Shen, Y.F., 2006. Development and characterisation of direct laser sintering multicomponent Cu based metal powder. *Powder Metallurgy*. 49, 258-264.
- Gu, D.D. and Shen, Y.F., 2009. Microstructures of Laser Sintered Micron/Nano-Sized Cu-W Powder. *Acta Metallurgica Sinica*. 45, 113-118.
- Gu, D.D., Shen, Y.F., Yang, J.L. and Wang, Y., 2006. Effects of processing parameters on direct laser sintering of multicomponent Cu based metal powder. *Materials Science and Technology*. 22, 1449-1455.
- Liu, Z.H., Zhang, D.Q., Chua, C.K. and Leong, K.F., 2013. Crystal structure analysis of M2 high speed steel parts produced by selective laser melting. *Materials Characterization*. 84, 72-80.
- Lockyer, S.A. and Noble, F.W., 1994. Precipitate structure in a Cu-Ni-Si alloy. *Journal of Materials Science*. 29, 218-226.
- Loh, L.E., Liu, Z.H., Zhang, D.Q., Mapar, M., Sing, S.L., Chua, C.K. and Yeong, W.Y., 2014. Selective Laser Melting of aluminium alloy using a uniform beam profile. *Virtual and Physical Prototyping*. 9, 11-16.
- Pogson, S.R., Fox, P., Sutcliffe, C.J. and O'Neill, W., 2003. The production of copper parts using DMLR. *Rapid Prototyping Journal*. 9, 334-343.
- Srivastava, V.C., Schneider, A., Uhlenwinkel, V., Ojha, S.N. and Bauckhage, K., 2004. Age-hardening characteristics of Cu-2.4Ni-0.6Si alloy produced by the spray forming process. *Journal of Materials Processing Technology*. 147, 174-180.
- Vijayaraghavan, V. and Wong, C.H., 2013. Shear deformation characteristics of single walled carbon nanotube with water interactions by using molecular dynamics simulation. *Physica E: Low-dimensional Systems and Nanostructures*. 54, 206-213.
- Vijayaraghavan, V. and Wong, C.H., 2013. Nanomechanics of single walled carbon nanotube with water interactions under axial tension by using molecular dynamics simulation. *Computational Materials Science*. 79, 519-526.
- Vijayaraghavan, V. and Wong, C.H., 2013. Temperature, defect and size effect on the elastic properties of imperfectly straight carbon. *Computational Materials Science*. 71, 184-191.
- Wang, C.C. and Wong, C.H., 2011. Short-to-medium range order of Al-Mg metallic glasses studied by molecular dynamics simulations. *Journal of Alloys and Compounds*. 509, 10222-10229.
- Wang, C.C. and Wong, C.H., 2012. Different icosahedra in metallic glasses: stability and response to shear transformation. *Scripta Materialia*. 66, 610-613.
- Wang, C.C. and Wong, C.H., 2012. Interpenetrating networks in Zr-Cu-Al and Zr-Cu metallic glasses," *Intermetallics*. 22, 13-16.
- Wang, C.C. and Wong, C.H., 2012. Structural properties of $Zr_xCu_{90-x}Al_{10}$ metallic glasses investigated by molecular dynamics simulations. *Journal of Alloys and Compounds*. 510, 107-113.
- Wong, C.H., Vijayaraghavan, V., 2014. Compressive characteristics of single walled carbon nanotube with water interactions investigated by using molecular dynamics simulation. *Physics Letter A*. 378, 570-576.
- Wong, C.H. and Vijayaraghavan, 2012. Nanomechanics of free form and water submerged single layer graphene sheet under axial tension by using molecular dynamics simulation. *Materials Science & Engineering A*. 556, 420-428.
- Wong, C.H. and Vijayaraghavan, 2012. Nanomechanics of non-ideal single and double walled carbon nanotubes. *Journal of Nanomaterials*. 2012, Article ID 490872.
- Wong, C.H. and Vijayaraghavan, 2012. Nanomechanics of imperfectly straight single walled carbon nanotubes under axial compression by using molecular dynamics simulation. *Computational Materials Science*. 53, 268-277.

- Wong, C.H., 2010. Elastic properties of imperfect single-walled carbon nanotubes under axial tension. *Computational Materials Science*. 49, 143-147.
- Zhang, D.Q., Liu, Z.H. and Chua, C.K., 2013. Investigation on forming process of copper alloys via Selective Laser Melting. *VRAP 2013*. Taylor & Francis Group, London, Portugal, pp. 285-289.
- Zhao, D.M., Dong, Q.M., Liu, P., Kang, B.X., Huang, J.L. and Jin, Z.H., 2003. Structure and strength of the age hardened Cu–Ni–Si alloy. *Materials Chemistry and Physics*. 79, 81-86.